ACS APPLIED MATERIALS & INTERFACES

Research Article

www.acsami.org

In Situ X-ray Near-Edge Absorption Spectroscopy Investigation of the State of Charge of All-Vanadium Redox Flow Batteries

Chuankun Jia,[†,§] Qi Liu,[†,§] Cheng-Jun Sun,[‡] Fan Yang,[†] Yang Ren,[‡] Steve M. Heald,[‡] Yadong Liu,[†] Zhe-Fei Li,[†] Wenquan Lu,[∥] and Jian Xie*[,†]

[†]Department of Mechanical Engineering, Purdue School of Engineering and Technology, Indiana University-Purdue University, Indianapolis, Indiana 46202, United States

[‡]X-ray Science Division, Advanced Photon Source, Argonne National Laboratory, 9700 S. Cass Ave., Argonne, Illinois 60439, United States

[∥]Chemical Science and Engineering Division, Argonne National Laboratory, 9700 S. Cass Ave., Argonne, Illinois 60439, United States

Supporting Information

ABSTRACT: Synchrotron-based *in situ* X-ray near-edge absorption spectroscopy (XANES) has been used to study the valence state evolution of the vanadium ion for both the catholyte and anolyte in all-vanadium redox flow batteries (VRB) under realistic cycling conditions. The results indicate that, when using the widely used charge−discharge profile during the first charge process (charging the VRB cell to 1.65 V under a constant current mode), the vanadium ion valence did not reach V(V) in the catholyte and did not reach V(II) in the anolyte. Consequently, the state of charge (SOC) for the VRB cell was only 82%, far below the desired 100% SOC. Thus, such incompletely charged mix electrolytes results in not only wasting the electrolytes but also decreasing the cell performance in the following cycles. On the basis of our study, we proposed a new charge−discharge profile (first charged at a constant current mode up to 1.65 V and then continuously charged at a constant voltage mode until the capacity was close to the theoretical value) for the first charge process that achieved 100% SOC after the initial charge process. Utilizing this new charge−discharge profile, the theoretical charge capacity and the full utilization of electrolytes has been achieved, thus having a significant impact on the cost reduction of the electrolytes in VRB.

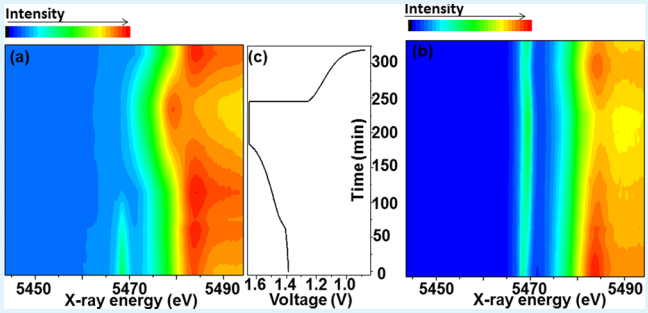

KEYWORDS: *all-vanadium flow battery, X-ray near-edge adsorption spectroscopy, synchrotron, in situ, state of charge, electrolyte*

1. INTRODUCTION

Redox flow batteries (RFBs) have been considered as one of the most promising technologies for large-scale intermittently renewable energy storage due to its high storage capacity, separate storage for energy and power, flexible design, and long cycle life.[1,2] A typical RFB cell consists of two electrodes separated by an ion-conducting membrane and two electrolyte reservoirs which circulate electrolyte solutions on each electrode.[1,3−6]Typically, when the RFB is charging, energy is stored; consequently, ions are reduced at the anode while ions are oxidized on the cathode in the RFB cell. Hence, there are always two electrolyte solutions comprising the different redox couples in the RFB system. Among different types of RFBs, the all-vanadium redox flow battery (VRB) displays excellent electrochemical activity and reversibility.[6−10] Unlike other redox flow batteries, a VRB uses the VO^{2+}/VO_2^+ redox couple in the positive half-cell and the V^{2+}/V^{3+} redox couple in the negative half-cell as shown in the following (charge process):[11]

Cathode:

$$VO^{2+} + H_2O \rightarrow VO_2^+ + 2H^+ + e^- \quad E^0 = 0.99\,V\,(vs.\,SHE) \qquad (1)$$

Anode:

$$V^{3+} + e^- \rightarrow V^{2+} \quad E^0 = -0.26\,V\,(vs.\,SHE) \qquad (2)$$

Overall reaction:

$$VO^{2+} + H_2O + V^{3+} \rightarrow VO_2^+ + 2H^+ + V^{2+} \quad E^0 = 1.25\,V \qquad (3)$$

Using the redox couples in both catholyte and anolyte can significantly eliminate the cross-contamination effect from different metals between the electrolytes through the membrane and thus reduce the self-discharge of battery. So until now, the VRB has the most promising potential for commercialization[9,12] compared to other flow batteries. However, the high cost of electrolytes and membranes still hinders its commercialization. In terms of the electrolytes, the most widely used vanadium material to prepare electrolytes is either $VOSO_4$ or V_2O_5. In order to reduce the cost of the electrolyte, different amounts of vanadium material with

Received: July 15, 2014
Accepted: September 5, 2014
Published: September 5, 2014

organic or inorganic additives have been studied to improve solubility and stability of the electrolyte solutions.[13,14] In addition, increasing the utilization of electrolytes is also an effective way to reduce the cost of electrolytes. The state of charge (SOC) of VRB depends on the oxidation state of the ions in the electrolyte. The accurate determination of the SOC at different oxidation states of ions is critical for the utilization of the electrolyte. However, until now, there have been no reports on the *in situ* investigation of the relationship between the SOC and the valence state of the electrolytes. Meanwhile, the utilization of the initial electrolytes is still unclear due to both the difficulty of monitoring the SOC and to the limited characterization methods resulting from the poor stability of the vanadium ions exposed to air (i.e., V^{2+} ions are easily oxidized into V^{3+} in the air[15]). In order to develop new electrolyte solutions for the next generation of VRB with lower cost, higher energy density, and longer cycle life, an in-depth understanding of the relationship between the oxidation state/local structure changes of the electrolytes and the electrochemical performance is critical. Therefore, *in situ* spectroscopic techniques are needed to monitor and study the local structure changes of the electrolytes during electrochemical cycling. Synchrotron radiation-based X-ray adsorption spectroscopy (XAS) is very informative when used to probe the environment around atoms of all states of matter.[16] The X-ray absorption near-edge structure (XANES) is especially powerful to determine the average oxidation state and local symmetry of the elements in all phases. With these considerations in mind, we carried out *in situ* XANES measurements during the cycling of a VRB single cell. To the best of our knowledge, this is the first report to use the *in situ* synchrotron techniques to study the redox flow battery. Here, we report our work on investigating the valence state changes of vanadium ions that occur in both the anolyte and the catholyte of the VRB during the initial charge/discharge process using *in situ* synchrotron XANES techniques. This advanced technique provides a nonintrusive, real-time monitoring of the changes that occur within the electrolytes under real operating conditions.

2. EXPERIMENTAL SECTION

2.1. Electrolyte and VRB. The all-vanadium electrolyte for both sides was initially made by dissolving 1.5 M $VOSO_4$ in a 2.0 M sulfuric acid solution. The homemade VRB single cells were used for this experiment as it can be seen in Figure S1, Supporting Information. For the batteries, conductive plastic plates served as the current collectors, carbon felt served as the electrodes, and a Nafion 112 membrane served as the separator. The active area of the electrode was 28 cm^2. The detailed description about the flow battery setup has been shown in the Supporting Information. To avoid overcharging the catholyte in the positive side, the volume of the catholyte was initially 160 mL, which was twice that of the anolyte (80 mL). After the first charge process, half of the catholyte solution was removed from the reservoir, making the volumes of both sides equal.

2.2. *In Situ* XANES Characterization during Electrochemical Cycling. A VRB single cell was cycled and *in situ* characterized under a new charge/discharge profile. The experiment setup for the *in situ* XANES study is shown in Figure 1a, and a scheme on this setup has been shown in Figure 1b for an easier understanding. The VRB single cell was placed on the stage of the beamline. Both the positive tank and negative tank are connected to the VRB single cell with the chemical resistant PVC tubes, among which there exist a small fraction of kapton tubes for X-rays. The X-ray beam was penetrating through the kapton tube from one side to the other side, and XANES patterns were collected. The VRB single cell was charged at a constant current

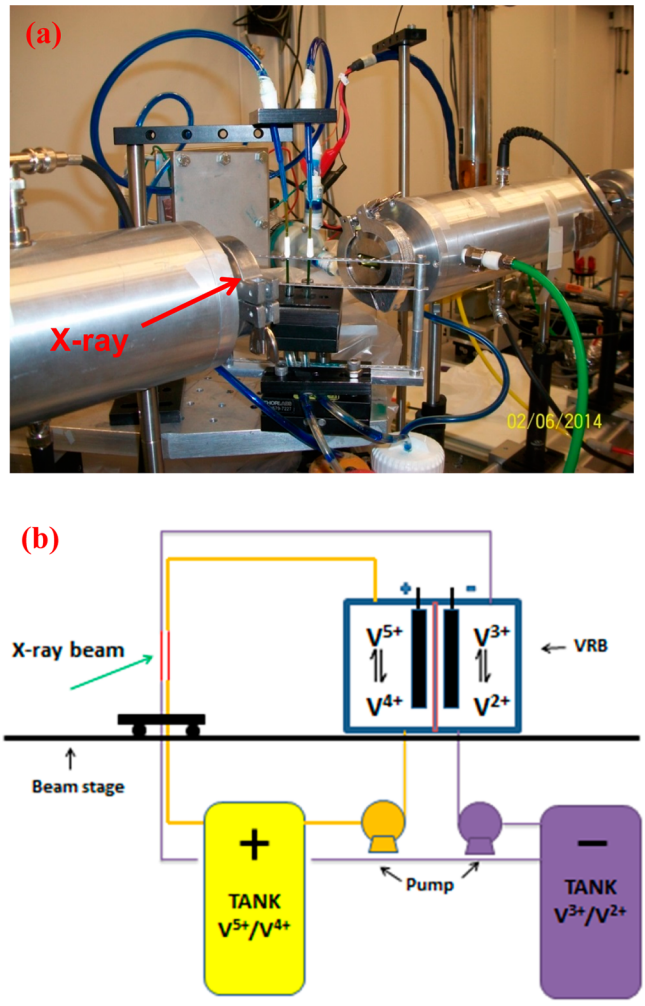

Figure 1. (a)The digital photo and (b) the scheme of the experiment setup for *in situ* synchrotron XANES experiment on all VRB flow batteries.

density (60 mA·cm^{-2}) up to 1.65 V (the same as the conventional profile) and, then, was continuously charged at a constant voltage of 1.65 V until the capacity was close to the theoretical value (3216.6 mAh for an 80 mL electrolyte), which is regarded as a 100% state of charge (SOC). Then, the cell was discharged at a constant current mode (60 mA·cm^{-2}) until the voltage reached 0.75 V. *In situ* XANES characterization was performed at the K-edge of the vanadium to monitor the change of the valence state of vanadium ions in both the anolyte and the catholyte. The XANES measurements were carried out in fluorescence mode at the beamline 20-BM of Advanced Photon Source, Argonne National Laboratory, using a Si (111) monochromator. Energy calibration was performed using the first derivative point of the XANES spectrum for V (K-edge = 5463.76 eV). The energy calibration was monitored for each *in situ* spectrum using vanadium metal foil in the reference channel. The spectra data were collected every 6 min. The XANES data reduction and analysis followed standard methods using the ATHENA software package.[17]

3. RESULTS AND DISCUSSION

The 1.5 M $VOSO_4$ in a 2.0 M sulfuric acid solution was initially placed in both the anolyte and the catholyte. In order to construct the redox couples for VRB, the initial VO^{2+} ions in the anolyte needed to be converted into V^{2+} ions, while the initial VO^{2+} ions in the catholyte needed to be changed to VO_2^+ ions; then, the VRB cell was in a fully charged state, namely, 100% SOC. Hence, the first charge process of the VRB

involved the reduction of VO^{2+} into V^{2+} ions on the anode side and the oxidation of VO^{2+} into VO_2^+ ions on the cathode side according to the following:

Anode side:

$$2H^+ + VO^{2+} + 2e^- \rightarrow V^{2+} + H_2O \quad (4)$$

Cathode side:

$$VO^{2+} + H_2O \rightarrow VO_2^+ + 2H^+ + e^- \quad (5)$$

Note that the anode side reduction (4) needs 2 electrons: 2 times the electrons needed on the cathode side (5). It was expected that the oxidation state of vanadium would be gradually reduced from +4 to +2 on the anode side, while being increased from +4 to +5 on the cathode side when the first charge process proceeded, and at the end of the charge process, all of the vanadium on the anode side should be in the +2 valence state, and the vanadium on the cathode side should all be in the +5 valence state. The current widely used method for converting V(IV) to V(V) and V(II) is to charge the VRB cell at a constant current mode to 1.65 V, regarded as the completion of the conversion[7,18,19] (we refer to this as the conventional charge profile). The choice of 1.65 V is based on the consideration of potentials of each electrode, the IR drop from the current flowing through the electrolyte, the contact resistance, and the limitation of the water electrolysis. Presumably, at 1.65 V, all V(IV) ions completely convert to V(V) ions and to V(II) ions, respectively. To investigate whether the completion is achieved, in this work, the VRB cell first was charged at a constant current mode to 1.65 V and, then, continued to charge at a constant voltage (i.e., 1.65 V) mode until the total Coulombs (required for reduction and oxidation) were achieved (we refer to this as the new charge profile).

3.1. *In Situ* XANES Study. 2D contour plots of XANES spectra for both anolyte and catholyte have been presented in Figure 2 to better illustrate the XANES spectra evolution

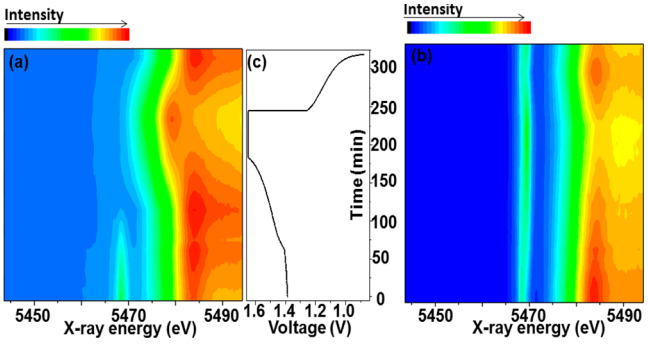

Figure 2. 2D contour plot of vanadium K-edge XANES spectra during the 1st charge/discharge process: (a) negative side, (b) positive side, and (c) voltage profile during the 1st charge/discharge process.

during the first charge process. In addition, the VRB voltage profile in the first charge/discharge process is displayed in the middle of the XANES spectra (Figure 2c). Obviously, the electrochemical process for both sides is well correlated with the evolution of the XANES data. For example, the inflection point observed in the contour plot of the XANES data coincides well with the critical point in the fully charged state around 240 min. The precipitous voltage drop from 1.65 V around 240 min corresponds to the beginning of the first discharge process.

The spectra of vanadium XANES during the first charge process is shown in Figure 3a,b. During the first charge process,

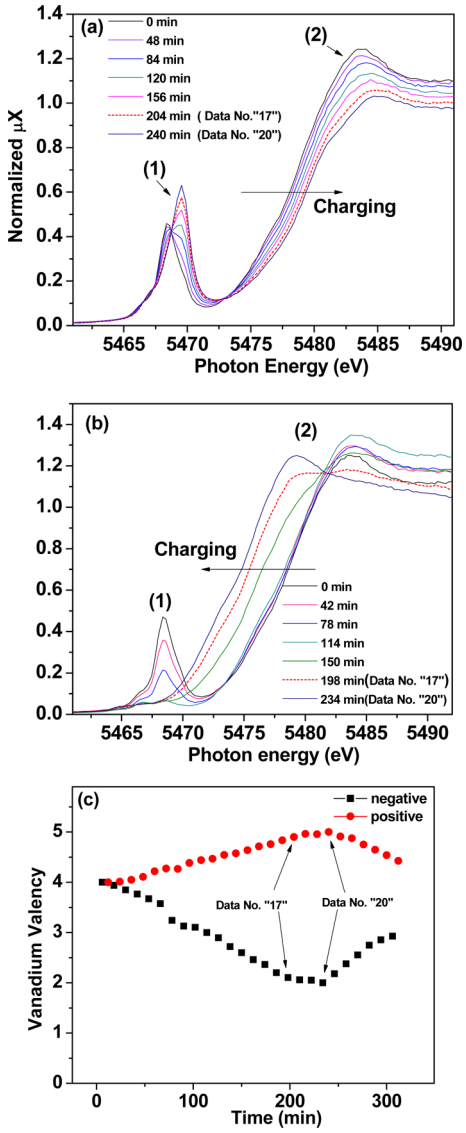

Figure 3. Typical vanadium XANES spectra show the evolution during the first charge process: (a) positive side; (b) negative side. (c) The vanadium valence evolution as the charging time. The data point for each side was recorded every 12 min. For the positive side: Data No. "17" (204 min); Data No. "20" (240 min). For negative side: Data No. "17" (198 min); Data No. "20" (234 min).

the electrolytes were charged under a constant current mode until the cell voltage reached 1.65 V and then were continuously charged under the constant voltage (i.e., 1.65 V) until the total Coulombs required for converting all V(IV) to V(V) (reaction 5) and all V(IV) to V(II) (reaction 4), respectively, were reached. Consequently, in the positive half-cell, the K-edge of the vanadium continuously shifted toward the higher binding energy. This shift is indicative of an increase in the average valence state of vanadium ions in the electrolyte (Figure 3a). The K-edge of the vanadium shifted back to the lower binding energy during the discharge process, which indicates a decrease in the average valence state of vanadium in

dx.doi.org/10.1021/am5046422 | ACS Appl. Mater. Interfaces 2014, 6, 17920−17925

the electrolyte (Figure S2, Supporting Information). Meanwhile, in the negative half-cell, the K-edge of vanadium continuously shifted toward lower binding energy during the charge process (Figure 3b), while it shifted back during the discharge process (Figure S2, Supporting Information). In addition to the K-edge, there are other important features in the XANES region: the pre-edge (labeled 1 in Figure 3) and the edge resonance (labeled 2 in Figure 3), which are also sensitive to the effective oxidation state of the vanadium and the chemical environment surrounding the vanadium site.[20] In the positive half-cell, the catholyte is typified by a strong 1s → 3d pre-edge absorption. In the strong acid solution, both V(V) and V(IV) exist in the hydrated form, which is a typical coordinated octahedral structure coordinated with related oxygen atoms and complex water molecules.[21] Since the intensity and position of the pre-edge is directly correlated to the distortion of the coordinated octahedral structure,[20] during the charge process, the pre-edge peak was observed to increase in the intensity and to shift toward higher energy (Figure 3a). In the negative half-cell, initially, the anolyte was charged from V(IV) to V(II), so the intensity of the pre-edge will continue to decrease as seen in Figure 3b. Theoretically, the strength of the pre-edge is found to be strongly dependent on the size of the "molecular cage" defined by the nearest neighbor ligands coordinating to the vanadium center. Consequently, unlike the VO^{2+}/VO_2^+ redox couple, the V^{2+}/V^{3+} redox couple has a very weak pre-edge absorption. During the discharge process, both the intensity and position of the pre-edge in VO^{2+}/VO_2^+ and the V^{2+}/V^{3+} redox couples (Figure S2, Supporting Information) showed a reversible change. A similar behavior of pre-edge evolution has been observed in crystalline V_2O_5 and V_2O_5 xerogel during the lithium insertion/deinsertion process.[22−25] In the XANES region, the intensity and shape of the edge resonance was found to be strongly related to the symmetry of the coordinating atoms surrounding the vanadium sites. This effect will be discussed in a separate publication in the near future. However, the reversible changes in intensity and position of edge resonance have also been observed for both the negative side and the positive side, which strongly confirms the local structure reversibility of the electrolyte.

The vanadium valence of electrolytes at different states of charge can be determined using a linear combination fitting by selecting XANES spectra of the starting materials and the end products.[16] The spectra were well fitted, with details of the standards selection procedure, and an example of a good fit was plotted and is discussed in Figures S3−S5, Supporting Information. To better illustrate the vanadium valence evolution in the process of the first charge, the derived vanadium valence from the XANES data in Figure 2a,c was plotted against the different charge times in terms of time and is shown in Figure 3c (time interval between two data numbers is 12 min). It is surprisingly noticed that the average valence of the vanadium ion in the catholyte increased from +4.0 (Figure 3c, 0 min/beginning of the first charge process) to +4.8 (Figure 3c, data number 17/204 min, which corresponds to the time for reaching 1.65 V, a threshold for completion of the first charge process using the conventional charge profile). Meanwhile the average valence of the vanadium ion in the anolyte decreased from +4.0 (Figure 3c, 0 min) to +2.2 (Figure 3c, data number 17/198 min) at data point 17. These data reveal that the initial $VOSO_4$ electrolyte was not fully charged to V(V) in the positive half-cell and V(II) in the negative half-cell using the conventional charging profile. From the perspective of the charge balance, it is clear that the increase in the average valence state of the vanadium ions in the positive side requires a decrease in the average valence state of the vanadium ions in the negative side (the change of valence state of vanadium ion in the negative side = 2× the change of valence state of vanadium ion in the positive side because 1 electron is needed on the cathode side, while 2 electrons are needed on the anode side). The average valence of the vanadium ion in the catholyte continues to change after data number 17 and becomes V(V), while the average valence of the vanadium ion in the anolyte becomes V(II) at data number 20, which corresponds to the end of the charge process using the new charge profile. The important finding from this work is that, clearly, the commonly used charge−discharge profile during the first charge process was not enough to completely convert all V(IV) to V(V) and to V(II); hence, it did not lead to the full utilization of the expensive electrolyte. Consequently, a mix of the charged electrolyte of VO^{2+} and VO_2^+ was obtained and has significantly impacted the cell performance as discussed below.

3.2. VRB Single-Cell Performance. To investigate the impact of the first charge profiles on cell performance, two different profiles of the VRB single cell performance after the first charge were compared. The charge capacities of the VRB single cells cycled under the same charge/discharge profile but were charged under different profiles for the first charge and are illustrated in Figure 4a. The charge capacity of the VRB single cell based on the new profile in the second cycle (first working cycle of a VRB cell) is 3255 mAh due to being slightly overcharged, which is slightly higher than the theoretical value (i.e., 3216.6 mAh for 80 mL electrolyte) and much higher than that based on conventional profiles (i.e., 2903 mAh for 80 mL), a 12% improvement. The difference of charge capacity between

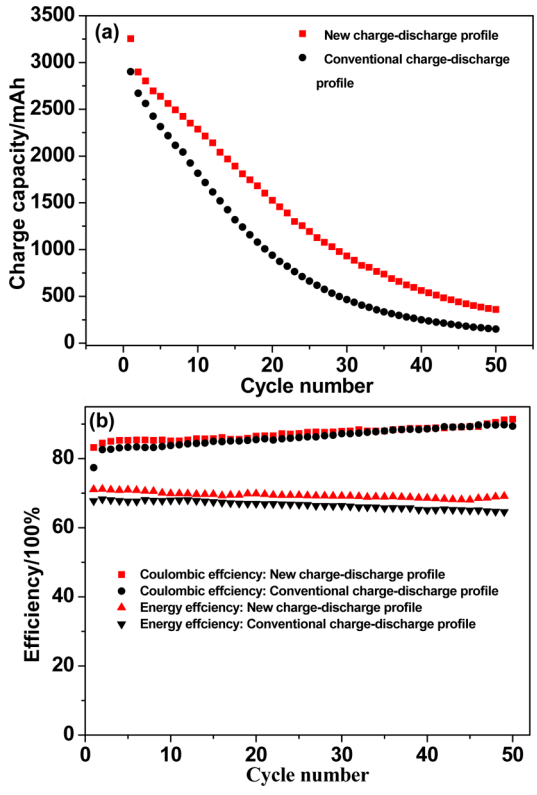

Figure 4. VRB single cell performance: (a) charge capacity and (b) efficiency.

dx.doi.org/10.1021/am5046422 | ACS Appl. Mater. Interfaces 2014, 6, 17920−17925

the cells with new and conventional first charge profiles increases with cycle number and reaches the maximum at about 20 cycles; then, the difference decreases with cycle number. Such a behavior could be due to two factors: (1) ions crossing over the membrane and (2) the amount of V(V) and V(II) on each side. After the first charge using the new profile, the VRB single cell began to cycle with complete V(V) on the cathode side and complete V(II) on the anode side. This leads to a lower ion crossover through the membrane[26] and higher electrolyte utilization and, consequently, a higher charge capacity. On the other hand, due to the mixed charged electrolytes resulting from using the conventional charge profile in the first charge process, the VRB cell starts cycling with the mixture of V(V) and V(IV) on the cathode side and V(II) and V(III) on the anode side, which leads to higher crossover and lower electrolyte utilization and, consequently, lower charge capacity. At 20 cycles, the electrolytes on both sides of the membrane reached the steady state, and the crossover was stabilized; thus, the charge capacity difference reached the maximum. After 20 cycles, the charge capacity became much smaller than the previous cycles; hence, the capacity difference became smaller with cycle number. The detailed mechanism of this behavior is under investigation and will be reported separately soon.

The VRB cells based on both profiles show obvious capacity loss. This may be due to the crossover of the vanadium ions and the self-discharge of the VRB cell. Further investigation of the capacity loss mechanism is ongoing using *in situ* XANES and *in situ* HEXRD and will be reported soon. The energy efficiency (EE) of the VRB single cell based on the new profile is slightly higher than that based on the conventional profile (71.0% vs 67.8% for the first cycle) and is accompanied by a slightly higher Coulombic efficiency (CE) (83.2% vs 77.4% for the first cycle). Thus, the new profile not only increases the capacity and energy but also increases the efficiency of the cell. The Coulombic efficiency increased with cycle number for the VRB single cells with both the first charge profiles. The decrease of charge capacity with cycle number was due to the use of the thin membrane (Nafion 212, 50 μm) and the cell structure,[27,28] while the self-discharge decreased much faster because the self-discharge was caused by the ion crossover. When the charge capacity was reduced, the corresponding time for charging was reduced as well; thus, the amount of ions crossing over the membrane during the period of charging were reduced, as was the self-discharge. Hence, an apparent increase in CE is observed. On the other hand, the high percentage of VO_2^+/VO^{2+} and V^{3+}/V^{2+} redox couples in both the positive and the negative sides (after charging with the new profile) improved the electrochemical activity and EE of the cell. There was a small increase of CE and no decrease of EE after 50 cycles, which indicates good stability for the VRB single cells based on both profiles.

On the basis of our results, we demonstrated that, using the conventional charge−discharge profile, the initial electrolyte (1.5 M $VOSO_4$ in 2 M sulfuric acid solution) was not fully oxidized to V(V) ions in the catholyte but was fully reduced to V(II) ions in the anolyte, respectively, which resulted in a waste of electrolytes and, consequently, lower SOC and lower cell performance. In order to fully utilize the electrolyte, a new charge−discharge profile during the first cycle was proposed. This new profile effectively increased the utilization of electrolytes to 100% and the initial cell capacity to the theoretical value in the first VRB single cell cycle. In addition, this study helps to better understand the correlation of electrolytes and the performance of the VRB. The new charge−discharge profile is an important step in reaching the goal of reducing the cost of the VRB system to less than $400 per kilowatt-hour.[12]

4. CONCLUSION

In summary, an *in situ* XANES technique has been used to investigate the valence changes of vanadium ions during the charge−discharge process in VRB cells for the first time. The intrinsic SOC of the cell can be monitored from the valence changes of the vanadium ions. The SOC obtained from the conventional charge−discharge profile in the first charge process is far from reaching 100%, which leads to the low utilization of electrolytes and a significant decrease in the cell performance in the following cycles. In this study, we designed a new charge−discharge profile for the first charge process. A VRB single cell reached a 100% SOC after being charged with this new profile in the first charge process. This new profile results in the increased utilization of electrolytes to 100% and improved cell performance. These results indicate that a VRB system cycling with an effective charge−discharge profile will be cost-effective and commercial application of the VRB system will be feasible in the near future. Furthermore, these results can also provide insights to further investigate the mechanisms in VRB systems using *in situ* XANES techniques and shed light on a variety of issues in other flow battery systems or other air-sensitive systems.

■ ASSOCIATED CONTENT

Ⓢ Supporting Information

In situ XANES spectrum during the 1st discharge process and the XANES spectra linear combination fitting standards procedure. This material is available free of charge via the Internet at http://pubs.acs.org/.

■ AUTHOR INFORMATION

Corresponding Author

*E-mail: jianxie@iupui.edu.

Author Contributions

§C.J. and Q.L. contributed equally.

Notes

The authors declare no competing financial interest.

■ ACKNOWLEDGMENTS

The PNC/XSD facilities at the Advanced Photon Source, and research at these facilities, are supported by the US Department of Energy - Basic Energy Sciences, the Canadian Light Source and its funding partners, the University of Washington, and the Advanced Photon Source. The use of the Advanced Photon Source, an Office of Science User Facility operated for the U.S. Department of Energy (DOE) Office of Science by Argonne National Laboratory, was supported by the U.S. DOE under Contract No. DE-AC02-06CH11357.

■ REFERENCES

(1) Wang, W.; Luo, Q.; Li, B.; Wei, X.; Li, L.; Yang, Z. Recent Progress in Redox Flow Battery Research and Development. *Adv. Funct. Mater.* **2013**, *23*, 970−986.

(2) Yang, Z.; Zhang, J.; Kintner-Meyer, M. C. W.; Lu, X.; Choi, D.; Lemmon, J. P.; Liu, J. Electrochemical Energy Storage for Green Grid. *Chem. Rev.* **2011**, *111*, 3577−3613.

(3) Huskinson, B.; Marshak, M. P.; Suh, C.; Er, S.; Gerhardt, M. R.; Galvin, C. J.; Chen, X.; Aspuru-Guzik, A.; Gordon, R. G.; Aziz, M. J. A Metal-Free Organic-Inorganic Aqueous Flow Battery. *Nature* **2014**, *505*, 195−198.
(4) Skyllas-Kazacos, M.; Rychcik, M.; Robins, R. G.; Fane, A. G.; Green, M. A. New All-Vanadium Redox Flow Cell. *J. Electrochem. Soc.* **1986**, *133*, 1057−1058.
(5) Wang, W.; Kim, S.; Chen, B.; Nie, Z.; Zhang, J.; Xia, G.-G.; Li, L.; Yang, Z. A New Redox Flow Battery Using Fe/V Redox Couples in Chloride Supporting Electrolyte. *Energy Environ. Sci.* **2011**, *4*, 4068−4073.
(6) Weber, A.; Mench, M.; Meyers, J.; Ross, P.; Gostick, J.; Liu, Q. Redox Flow Batteries: A Review. *J. Appl. Electrochem.* **2011**, *41*, 1137−1164.
(7) Jia, C.; Liu, J.; Yan, C. A Significantly Improved Membrane for Vanadium Redox Flow Battery. *J. Power Sources* **2010**, *195*, 4380−4383.
(8) Li, L.; Kim, S.; Wang, W.; Vijayakumar, M.; Nie, Z.; Chen, B.; Zhang, J.; Xia, G.; Hu, J.; Graff, G.; Liu, J.; Yang, Z. A Stable Vanadium Redox-Flow Battery with High Energy Density for Large-Scale Energy Storage. *Adv. Energy Mater.* **2011**, *1*, 394−400.
(9) Rahman, F.; Skyllas-Kazacos, M. Vanadium Redox Battery: Positive Half-Cell Electrolyte Studies. *J. Power Sources* **2009**, *189*, 1212−1219.
(10) Service, R. F. Tanks for the Batteries. *Science* **2014**, *344*, 352−354.
(11) Li, X.; Zhang, H.; Mai, Z.; Zhang, H.; Vankelecom, I. Ion Exchange Membranes for Vanadium Redox Flow Battery (VRB) Applications. *Energy Environ. Sci.* **2011**, *4*, 1147−1160.
(12) Zhang, H. Rechargeables: Vanadium Batteries Will Be Cost-effective. *Nature* **2014**, *508*, 319−319.
(13) Liang, X.; Peng, S.; Lei, Y.; Gao, C.; Wang, N.; Liu, S.; Fang, D. Effect of L-Glutamic Acid on the Positive Electrolyte for All-Vanadium Redox Flow Battery. *Electrochim. Acta* **2013**, *95*, 80−86.
(14) Skyllas-Kazacos, M.; Peng, C.; Cheng, M. Evaluation of Precipitation Inhibitors for Supersaturated Vanadyl Electrolytes for the Vanadium Redox Battery. *Electrochem. Solid-State Lett.* **1999**, *2*, 121−122.
(15) Schwenk, C. F.; Loeffler, H. H.; Rode, B. M. Structure and Dynamics of Metal Ions in Solution: QM/MM Molecular Dynamics Simulations of Mn^{2+} and V^{2+}. *J. Am. Chem. Soc.* **2003**, *125*, 1618−1624.
(16) Cui, Y.; Abouimrane, A.; Lu, J.; Bolin, T.; Ren, Y.; Weng, W.; Sun, C.; Maroni, V. A.; Heald, S. M.; Amine, K. (De)Lithiation Mechanism of Li/SeS_x (x = 0−7) Batteries Determined by *in Situ* Synchrotron X-ray Diffraction and X-ray Absorption Spectroscopy. *J. Am. Chem. Soc.* **2013**, *135*, 8047−8056.
(17) Ravel, B.; Newville, M. ATHENA, ARTEMIS, HEPHAESTUS: Data Analysis for X-ray Absorption Spectroscopy using IFEFFIT. *J. Synchrotron Radiat.* **2005**, *12*, 537−541.
(18) Park, M.; Jung, Y.-j.; Kim, J.; Lee, H. i.; Cho, J. Synergistic Effect of Carbon Nanofiber/Nanotube Composite Catalyst on Carbon Felt Electrode for High-Performance All-Vanadium Redox Flow Battery. *Nano Lett.* **2013**, *13*, 4833−4839.
(19) Qian, P.; Zhang, H.; Chen, J.; Wen, Y.; Luo, Q.; Liu, Z.; You, D.; Yi, B. A Novel Electrode-Bipolar Plate Assembly for Vanadium Redox Flow Battery Applications. *J. Power Sources* **2008**, *175*, 613−620.
(20) Wong, J.; Lytle, F. W.; Messmer, R. P.; Maylotte, D. H. K-edge Absorption Spectra of Selected Vanadium Compounds. *Phys. Rev. B* **1984**, *30*, 5596−5610.
(21) Vijayakumar, M.; Burton, S. D.; Huang, C.; Li, L.; Yang, Z.; Graff, G. L.; Liu, J.; Hu, J.; Skyllas-Kazacos, M. Nuclear Magnetic Resonance Studies on Vanadium(IV) Electrolyte Solutions for Vanadium Redox Flow Battery. *J. Power Sources* **2010**, *195*, 7709−7717.
(22) Giorgetti, M.; Passerini, S.; Smyrl, W. H.; Mukerjee, S.; Yang, X. Q.; McBreen, J. *In Situ* X-Ray Absorption Spectroscopy Characterization of V 2 O 5 Xerogel Cathodes upon Lithium Intercalation. *J. Electrochem. Soc.* **1999**, *146*, 2387−2392.
(23) Huguenin, F.; Ticianelli, E. A.; Torresi, R. M. XANES Study of Polyaniline−V_2O_5 and Sulfonated Polyaniline−V_2O_5 Nanocomposites. *Electrochim. Acta* **2002**, *47*, 3179−3186.
(24) Liu, Q.; Liu, Y.; Sun, C.-J.; Li, Z.-f.; Ren, Y.; Lu, W.; Stach, E. A.; Xie, J. The Structural Evolution of V_2O_5 Nanocystals during Electrochemical Cycling Studied Using *In operando* Synchrotron Techniques. *Electrochim. Acta 136*, 318−322.
(25) Mansour, A. N.; Smith, P. H.; Baker, W. M.; Balasubramanian, M.; McBreen, J. *In Situ* XAS Investigation of the Oxidation State and Local Structure of Vanadium in Discharged and Charged V_2O_5 Aerogel Cathodes. *Electrochim. Acta* **2002**, *47*, 3151−3161.
(26) Xi, J.; Wu, Z.; Qiu, X.; Chen, L. Nafion/SiO_2 Hybrid Membrane for Vanadium Redox Flow Battery. *J. Power Sources* **2007**, *166*, 531−536.
(27) Schwenzer, B.; Kim, S.; Vijayakumar, M.; Yang, Z.; Liu, J. Correlation of Structural Differences between Nafion/polyaniline and Nafion/polypyrrole Composite Membranes and Observed Transport Properties. *J. Membr. Sci.* **2011**, *372*, 11−19.
(28) Kim, S.; Yan, J.; Schwenzer, B.; Zhang, J.; Li, L.; Liu, J.; Yang, Z.; Hickner, M. A. Cycling Performance and Efficiency of Sulfonated Poly(sulfone) Membranes in Vanadium Redox Flow Batteries. *Electrochem. Commun.* **2010**, *12*, 1650−1653.